

SUB-MICROKELVIN PRECISION THERMAL CONTROL SYSTEM USING MODEL PREDICTIVE ALGORITHM FOR LASER INTERFEROMETER SPACE ANTENNA GROUND VERIFICATION FACILITY

Sei Higuchi¹, Daniel B. DeBra¹, and Steve Rock¹

¹Department of Aeronautics and Astronautics
Stanford University
Stanford, CA, U.S.A.

INTRODUCTION

Laser Interferometer Space Antenna (LISA) aims to detect directly gravitational waves from massive black holes and galactic binaries. LISA is essentially a massive Michelson interferometer placed in space with a third spacecraft added. In Einstein's theory of general relativity, the gravity is due to curvature of spacetime, which is caused by the presence of massive objects. The gravitational waves are ripples in spacetime. As the waves reaching to the vicinity of the Earth pass through the LISA spacecraft, the fractional change in interferometer arm length can be as small as $10^{-21} m/m\sqrt{Hz}$ even for the powerful sources. LISA will monitor fractional changes in the light-travel times across arms of a nominally 5 million km. For this reason LISA requires gravitational reference sensors (GRS) for drag-free control [1] and will achieve the required sensitivity through minimizing spurious forces (non-gravitational-wave force), which come from both the environment and the spacecraft themselves. The total acceleration disturbance to each proof mass, which floats at the center of GRS, is required to be below $3 \times 10^{-15} m/s^2\sqrt{Hz}$. Optical path length variations on each optical bench must be kept below $40 pm/\sqrt{Hz}$ [2]. The job of the spacecraft is to shield an internal proof mass that falls freely, not attached to the spacecraft, from external disturbances.

Several sources contribute to the disturbances including magnetic force, cosmic rays, temperature fluctuations, residual gas pressure, and sensor disturbance [2]. This presentation focuses on minimizing the effects of thermal disturbances to the proof-mass (PM). Thermal effects seem to be an innocent problem to manage. However, limited thermal mass of the spacecraft and relatively low frequency range, they call for active compensation mechanism to satisfy the requirements particularly at low frequency range. P. L. Ben-

der [3] claims that the passive thermal isolation clearly will become worse at frequencies substantially below $0.1 mHz$ and suggests the need of active temperature control systems as well as larger gaps around the proof-mass: the current nominal gap size between PM and S/C is $2 mm$. The modular GRS (MGRS) has been proposed by the team from Stanford University with the suggested gap size of a few cm [4].

Thermal disturbances due to, for example, solar irradiation, or temperature gradients across the proof mass housing is expected to be significant disturbance source to the LISA sensitivity requirements of $\Delta T < 30 \mu K/\sqrt{Hz}$ over $0.1 mHz$ to $1 Hz$. Even a small temperature gradient can produce distortions in the housing structure, which results in a change in the mass attraction force [5]. Temperature fluctuations also cause radiometer effects with residual gas pressure as well as the net thermal radiation pressure.

Designing an active control system compensating low-frequency disturbance input is extremely challenging. First of all, the temperature stability requirement is significantly tighter compared to other types of thermal control requirements. The temperature profile of the spacecraft must be uniform to the order of $10^{-5} K/\sqrt{Hz}$ both temporally and spatially. Another challenging factor is the time-delay. The Smith-predictor [6] is a major control scheme that compensates time-delay. Because we are also interested in spatial temperature profile, the control system is required to manage multiple outputs as well as multiple inputs in the presence of constraints. Thus, the model predictive control (MPC) scheme is mainly discussed in this paper even though some of the experimental results were obtained through the Smith-predictor scheme.

We have developed a thermal control system for

LISA GRS. For ground testing, the LISA specification can be met fairly readily with massive amount of insulation and thermal mass. Since the ground testing facility is by extension suitable for in-flight thermal condition to compensate external forces, the test facility is designed to be analogous to the spacecraft structure. Continuing development of control algorithm and improvement of measurement resolution will extend performance to below than LISA coverage of super massive black hole mergers.

EXPERIMENTAL SYSTEM

Figure 1 shows a schematic figure of the experimental system. The various layers of insulation correspond in a rough way to the layers of thermal isolation provided by the LISA spacecraft design [7], although various adaptations were necessary to be consistent with resource availability. The

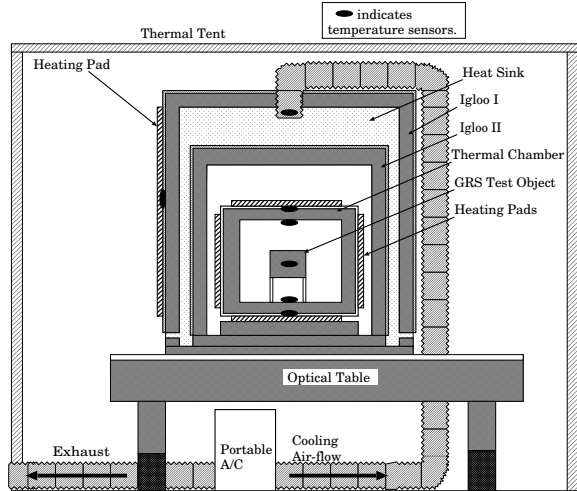


FIGURE 1. The schematic of the experimental system

GRS sensor test-object is placed in the center of a double walled thin metal thermal enclosure, analogous to the LISA internal shield. A precision thermistor monitors the test-object with ($< 100 \mu K/\sqrt{Hz}$) noise. The enclosure is wrapped in flexible insulation, and wrapped again with copper foil. This copper foil surface corresponds roughly to the LISA Y-tube surface, and here is temperature controlled to high-precision by a heating-pad/thermocouple feedback system. Surrounding the enclosure and heater-pad apparatus is 2" of foil-covered polystyrene foam insulation, labeled igloo1 and igloo2, to create a sealed control volumes. The outer surface of igloo2 is maintained by a temperature regulated air-flow system which removes waste heat, simulating for space will be

replaced with a cold radiator to deep space.

Six heating pads, our primary actuators, are driven with an AC power source. They are installed around the surfaces of thermal enclosure inside igloo2 and two are installed outside igloo1 to create artificial temperature disturbance inputs. Accordingly a variable controllable AC power supply is the most desired equipment. However, due to the limited availability, the experiment is being conducted utilizing a 24 Vac power source, the output level of which is fixed. Therefore, the control program first computes the numerical value of the heating pad temperature inputs (control signal) based on the desired final outputs and then sets as the value obtained as the reference track the reference of the control signal. Since the band width of the heating pad is significantly greater than that of the GRS, this scheme performs very well to emulate a smooth control input. Seven sensors are installed to measure the ambient temperature inside the thermal tent, the heating-pad temperatures, temperatures inside double-walled enclosure and the GRS test-object. Finally, the entire system is placed within a clear plastic thermal tent, primarily to cut down on air drafts.

A typical time history of the ambient and GRS test-object temperature is shown in Figure 2. The data was acquired without control authority and reveals significant coupling between the ambient and the GRS temperatures. Although the system has multiple layers of thermal insulation, the GRS test-object temperature is still varying roughly $\pm 0.2 K$, which is obviously too large fluctuation for the LISA requirement, $30 \mu K/\sqrt{Hz}$.

PLANT MODEL

The physical plant is modeled as a combination of a second-order plant is modeled as a combination of a second-order plant plus a single time-delay element. The model parameters are fitted empirically using least-square and MATLAB simulations. Our plant model with p inputs and q outputs is expressed in a state-space model.

$$\begin{aligned} x(k+1) &= Ax(k) + Bu(k-h) \\ y(k) &= Cx(k) + \zeta(k) \end{aligned} \quad (1)$$

where x is the n -dimensional state vector, u is the p -dimensional control input vector, h is the time-delay, w is the disturbance vector, ζ is the q -dimensional measurement noise vector, A , B , and C are system matrices with dimensions $n \times n$, $n \times p$, $n \times 1$, and $q \times n$, respectively.

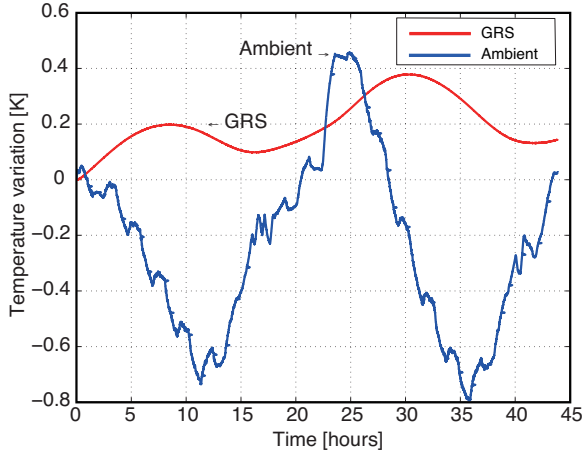


FIGURE 2. Time history of typical daily temperature variation

MODEL PREDICTIVE CONTROL

In this section, a MPC control law is developed for a general case of MIMO LTI systems. Figure 3 represents the control block diagram of the entire system. Feedback and feedforward control loops

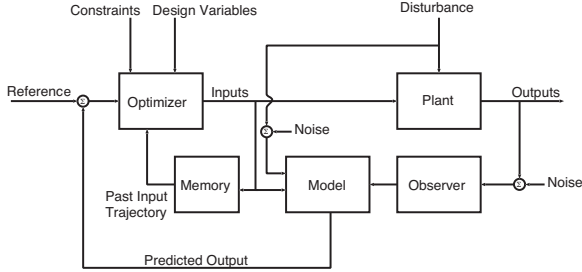


FIGURE 3. Control system block diagram

are formulated. The optimizer minimizes the cost function given by

$$J(k) = \|Y_d(k) - Y(k)\|_{\hat{Q}}^2 + \|\Delta U(k)\|_{\hat{R}}^2 \quad (2)$$

where $Y_d(k)$ is the $H_p \times q$ -dimensional reference trajectory, $Y(k)$ is the predicted outputs, $\Delta U(k)$ is the $H_p \times p$ -dimensional input sequence, \hat{Q} and \hat{R} are the weighting matrices. In order to compute the optimal control input by minimizing the cost function, predicted outputs need to be computed over the prediction horizon, H_p . The predicted outputs is given by

$$Y(k) = G(A - KC)x(k) + GK y(k) + F_1 U_p(k) + F_2 \Delta U(k) \quad (3)$$

where, K is the observer gain, $G = [C, CA, \dots, CA^{h+H_p}]^T$, $U_p(k) =$

$[u(k-h), \dots, u(k-1)]^T$ past input trajectory,

$$F_1 = \begin{bmatrix} CB & & & 0 \\ \vdots & \ddots & & \\ CA^{h-1}B & \dots & CAB & B \\ \vdots & & & \vdots \\ CA^{h+H_p}B & \dots & CA^{H_p+2}B & \sum_{i=0}^{p+1} CA^i B \end{bmatrix} \in \mathfrak{R}^{(h+H_p+1)q \times hp}$$

and

$$F_2 = \begin{bmatrix} 0 & \dots & & 0 \\ \vdots & \ddots & & \vdots \\ CB & \ddots & & \vdots \\ CAB + CB & \ddots & & \vdots \\ \vdots & \ddots & & 0 \\ \sum_{i=0}^p CA^i B & & CAB + CB & CB \end{bmatrix} \in \mathfrak{R}^{(h+H_p+1)q \times (H_p+1)p}$$

Using Eq.(3), the cost function can be expressed as a function of $\Delta U(k)$.

$$J(k) = \Delta U^T(k) H \Delta U(k) + 2b \Delta U(k) \quad (4)$$

where

$$H = F_2^T \hat{Q} F_2 + \hat{R}$$

$$b = E_k^T \hat{Q} F_2$$

$$E_k = Y_d(k) - G(A - KC)x(k) - GK y(k) - F_1 U_p(k)$$

Note that the constant term in Eq.(4) is omitted.

If no specific constraints is specified, the optimal input $\Delta U(k)$ is given by the least-square solution that minimizes the cost function Eq.(4).

$$\Delta U(k) = H^{-1} F_2^T \hat{Q} E_k \quad (5)$$

Otherwise, if constraints are present, the solution is given by quadratic programming. In order to add feedforward action to the controller, the internal model includes a dynamics of sinusoidal disturbance temperature, which is given by

$$\begin{aligned} x_d(k+1) &= A_d x_d(k) \\ w(k) &= C_d x_d(k) + \zeta_d(k) \end{aligned}$$

Moreover, the actual cost function account for the estimate of disturbance effect that is given by

$$d_{est}(k) = y_{plant}(k) - y_{model}(k) \quad (6)$$

and then the cost function is finally expressed by modifying the E_k :

$$E_k = Y_d(k) - G(A - KC)x(k) - GK y(k) - F_1 U_p(k) - d_{est} \vec{1} \quad (7)$$

where $\vec{1} \in \mathbb{R}^{(h+H_p+1)q \times 1}$. The weighting matrices \hat{Q} , \hat{R} , and the prediction horizon H_p are chosen so that the control law Eq.(5) is stabilized.

RESULTS

Figure 4 demonstrates the portion of 30-day simulation of the temperatures measured at the sensors together with the heating pad (input) and the ambient temperature (disturbance). The temperature is maintained approximately $\pm 25 \mu K$ over 30-day observation. As the daily ambient temperature cycles in 24 hours, the GRS is still affected by such a low frequency signal ($\sim 10^{-5} Hz$). During the simulation, the disturbance temperature was modeled as a sum of three sinusoidal waves, $d(t) = \sum_{i=1}^3 A_i \sin(\omega_i t + \phi_i)$. The mean squared

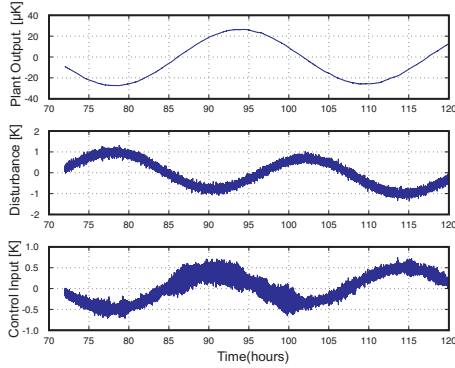


FIGURE 4. Time history of the GRS test-object, control input, and disturbance temperature power spectral density of temperature variations of the GRS test-object as well as some experimental data is presented in Figure 5. The temperature fluctuation is almost achieved below $30 \mu K / \sqrt{Hz}$ above $0.1 mHz$.

CONCLUDING REMARKS

The simulation and corresponding past thermal experiment results are presented. The result implies that the control law will attenuate temperature variation as low as by a factor of $10^4 \sim 10^5$. We are expecting to implement the control system in our laboratory and demonstrate experimental results at the annual meeting. In addition to continuing development of the control system, for the better precision, less noise and more long-term stability, improved measurement will be required to fully satisfy the LISA thermal requirement.

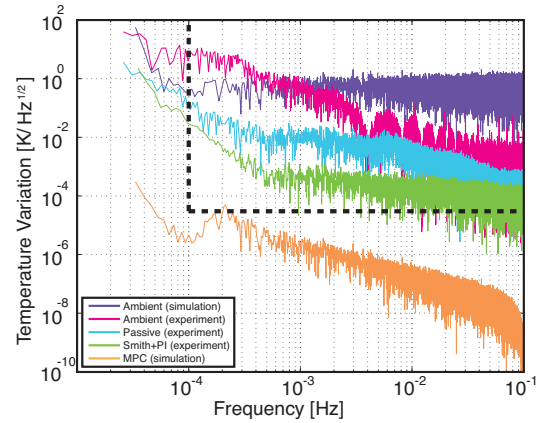


FIGURE 5. Thermal stability in the frequency domain (below of dashed lines indicates the LISA thermal requirement).

ACKNOWLEDGMENTS

This research was supported by NASA, NNX07AK65G, Modular Gravitational Reference Sensor for Space Gravitational Wave Detection.

REFERENCES

- [1] DeBra DB. Drag-free spacecraft as platforms for space missions and fundamental physics. *Class Quantum Grav.* 1997;14:1549–1555.
- [2] Schumaker BL. Disturbance reduction requirements for LISA. *Classical and Quantum Gravity.* 2003;20(10):S239–S253.
- [3] Bender PL. LISA sensitivity below $0.1 mHz$. *Class Quantum Grav.* 2001;20:S301–S310.
- [4] Ke-Xun Sun ea. Advanced gravitational reference sensor for high precision space interferometers. *Class Quantum Grav.* 2005;22(10):S287–S294.
- [5] Swank AJ. Gravitational mass attraction: properties of a right-angled parallelepiped for the LISA drag-free system. *Class Quantum Grav.* 2006;23:3437–3448.
- [6] Smith OJM. Closer Control of Loops with Dead Time. *Chemical Engineering Progress.* 1957;53:217–219.
- [7] Final Technical Report of the (Phase A) Study of the Laser Interferometer Space Antenna. 2000;.